Unusual nighttime impulsive *fo*F2 enhancement below the southern anomaly crest under geomagnetically quiet conditions

M. Pezzopane[1], P. R. Fagundes[2], L. Ciraolo[3], E. Correia[4], M. A. Cabrera[5,6,7], and R. G. Ezquer[6,7,8]

[1]Istituto Nazionale di Geofisica e Vulcanologia, Via di Vigna Murata 605, 00143, Rome, Italy

[2]Universidade do Vale do Paraíba, Física e Astronomia, Av. Shishima Hifumi, 2911, São José dos Campos, SP, Brazil

[3]IFAC-CNR, Via Madonna del Piano, 10, 50019, Florence, Italy

[4]Instituto Nacional de Pesquisas Espaciais, Centro de Radioastronomia e Astrofísica Mackenzie, Rua da Consolação, 896, São Paulo, SP, Brazil

[5]Laboratorio de Telecomunicaciones, DEEC, FACET, Universidad Nacional de Tucumán, Av. Independencia 1800, 4000 Tucumán, Argentina

[6]Laboratorio de Ionósfera, Dpto. de Física, FACET, Universidad Nacional de Tucumán, Av. Independencia 1800, 4000 Tucumán, Argentina

[7]CIASUR, Facultad Regional Tucumán, Universidad Tecnológica Nacional, Rivadavia 1050, 4000 Tucumán, Argentina

[8]Consejo Nacional de Investigaciones Científicas y Técnicas (CONICET), Rivadavia 1917, 1033 Buenos Aires, Argentina

Correspondence to: M. Pezzopane (michael.pezzopane@ingv.it)

Abstract

An unusual nighttime impulsive electron density enhancement was observed on the 6th of March 2010 over a wide region of South America, below the southern crest of the equatorial anomaly, under low solar activity and quiet geomagnetic conditions. The phenomenon was observed almost simultaneously by the F2 layer critical frequency (*fo*F2) recorded at three ionospheric stations which are widely distributed in space, namely: Cachoeira Paulista (22.4° S, 44.6° W, magnetic latitude 13.4° S), São José dos Campos (23.2° S, 45.9° W, magnetic latitude 14.1° S), [Brazil], and Tucumán (26.9° S, 65.4° W, magnetic latitude 16.8° S), [Argentina]. Although in a more restricted region over Tucumán, the phenomenon was also observed by the total electron content (TEC) maps computed by using measurements from twelve GPS receivers. The investigated phenomenon is very particular because besides being of brief duration, it is characterized by a pronounced compression of the ionosphere. This compression was clearly visible both by the virtual height of the base of the F layer (*h*'F) recorded at the aforementioned ionospheric stations, and by both the vertical electron density profiles and the slab thickness computed over Tucumán. Consequently, neither an enhanced fountain effect nor plasma diffusion from the plasmasphere can be considered as the single cause of this unusual event. A thorough analysis of isoheight and isofrequency ionosonde plots suggest that travelling ionospheric disturbances (TIDs) caused by gravity wave (GW) propagation could have likely played a significant role in causing the phenomenon.

Keywords: equatorial ionosphere; travelling ionospheric disturbance; ionosphere-atmosphere interactions; instrument and techniques

1. Introduction

Unlike the F1 and the E layers, the ionospheric F2 layer cannot be considered as a Chapman-layer due to its significant day-to-day variability, mostly in the equatorial anomaly region and at high latitudes. As a consequence, the F2 layer parameters, such as the F2 layer critical frequency (*fo*F2), the maximum electron density (*Nm*F2) and the height of *Nm*F2 (*hm*F2) often show significant deviation from climatological values. The *fo*F2 is related to the *Nm*F2 as $1.24 \cdot 10^{10} \cdot (foF2)^2$, where the units of *Nm*F2 and *fo*F2 are m^{-3} and MHz respectively.

Since day-to-day variability is fundamental for the development of ionospheric empirical models, several studies have been performed to reveal any trends in the ionospheric plasma function of different parameters like local time, season, and solar activity [e.g., *Kouris and Fotiadis*, 2002; *Ezquer et al*., 2004; *Liu et al*., 2009; *Akala et al*., 2010; *Borries and Hoffmann*, 2010; *Chen et al*., 2010; *David et al*., 2010; *Lin et al*., 2010; *Liu G. et al*., 2010; *Hall et al*., 2011; *He et al*., 2011; *Lee et al*., 2011; *Liu et al*., 2011].

Traditionally, ionospheric F2 layer disturbances have been linked to solar and geomagnetic activity variations. However, there are disturbances, termed "meteorological" by *Rishbeth and Mendillo* [2001], that seem to arise from the lower part of the atmosphere and hence are different from those triggered by geomagnetic activity. As a follow up to the work by *Rishbeth and Mendillo* [2001], *Mikhailov et al*. [2004] suggested the term "Q disturbances" to indicate, positive or negative, *Nm*F2 deviations greater than 40% if all 3-h *Ap* indices were ≤7 for the previous 24 hours. *Mikhailov et al*. [2004] and *Depueva et al*. [2005] illustrated the morphology of Q disturbances using data from 26 ionosondes in the northern hemisphere and only 2 around the geomagnetic equator. With regard to the Q disturbances, positive phases before the beginning of a geomagnetic storm, termed pre-storm enhancements, were recently investigated at middle latitudes by *Buresova and Laštovička* [2008] and at low latitudes by *Liu et al*. [2008a, b].

It is well-known that the nighttime values of *fo*F2 and total electron content (TEC) do not always decrease smoothly. Several authors performed statistical studies on *Nm*F2 and TEC enhancements at mid and low latitudes [*Janve et al*., 1979; *Balan and Rao*, 1987; *Lois et al*., 1990; *Balan et al*., 1991; *Balan et al*., 1994; *Su et al*., 1994; *Mikhailov et al*., 2000a; *Farelo et al*., 2002; *Pavlov and Pavlova*, 2007; *Luan et al*., 2008].

Su et al. [1994], using data from four stations in the northern equatorial anomaly regions, investigated the variations of the nighttime TEC enhancements with season, solar activity, latitude, and longitude. They showed that at equatorial anomaly latitudes there are two kinds of nighttime enhancement, a postsunset enhancement occurring at around 20:00 Local Time (LT) and a postmidnight enhancement occurring at around 01:00-02:00 LT. Postsunset enhancements were shown to be stronger and more frequent in autumn, and characterized by a frequency of occurrence, a mean amplitude and a mean half amplitude duration increasing as the solar activity increases. Postmidnight enhancements were shown to be stronger and more frequent at eastern longitudes than at western longitudes. With regard to the physical processes responsible for these enhancements, they confirmed that the primary source of the postsunset one is the prereversal enhancement of the equatorial fountain. Concerning the postmidnight enhancement, they attributed it to a delay of the reversal time of the **E**x**B** drift which, combined with the equatorward meridional neutral winds, causes an uplift of the F region to higher altitudes of lower chemical loss.

Mikhailov et al. [2000a] have specifically analyzed the postmidnight *Nm*F2 enhancements, and its possible mechanism of formation, using Millstone Hill Incoherent Scatter Radar observations and Boulder ionosonde *fo*F2 observations. They showed that the postmidnight peak occurrence is characterized by a well pronounced seasonal variation, being more frequent in winter both at solar minimum and maximum. Their conclusions concerning the physical process responsible for the formation of this postmidnight peak validated the previous findings by *Mikhailov and Förster* [1999],

who had shown that the main cause of these phenomena is the joint effect of equatorward thermospheric winds and downward electron plasmaspheric fluxes, which causes an *hm*F2 nighttime increase responsible for the *Nm*F2 peak. They also stated that the **E**x**B** drift is inefficient for the middle latitude *Nm*F2 nighttime peak formation at high solar activity.

Farelo et al. [2002] presented a detailed study of the morphology of *Nm*F2 nighttime enhancements, for different seasons and solar activity levels. They showed that postmidnight enhancements are smaller than the premidnight ones, and in general that the enhancements are characterized by a large upsurge at lower latitudes. The amplitude of the postmidnight peak was shown to have seasonal and solar activity dependences, being larger in winter and during low solar activity, while the times of occurrence were found to be similar to those found by *Su et al*. [1994]. They attributed the premidnight peak to the joint effect of the collapse in the F region due to the electron temperature decrease after sunset (which produces large downward electron fluxes) and equatorward meridional thermospheric winds (which produces an uplift of the F region to heights with low recombination rates), and the postmidnight peak to the joint effect of equatorward thermospheric winds and nighttime electron fluxes from the plasmasphere.

Pavlov and Pavlova [2007] conducted a statistical study on anomalous nighttime *Nm*F2 peaks measured by ionosondes close to the geomagnetic equator, and the most important thing they showed is that the probability of occurrence of the premidnight and postmidnight peaks depends on geomagnetic longitude.

Luan et al. [2008] investigated the nighttime enhancement morphology at mid latitudes in the northern hemisphere using COSMIC (Constellation Observing System for Meteorology, Ionosphere, and Climate) observations in an altitude range from 200 to 500 km, at solar minimum and under quiet geomagnetic conditions. They found that the enhancements in electron density are evident near the F2 layer peak, within 50-100 km of the F2 layer peak height, at most latitudes and longitudes. They did

not observe any obvious enhancements in the topside and bottom side of the ionosphere, even though significant electron density enhancements did occur. They attributed the longitudinal variations of the nighttime enhancements to different downward plasma fluxes, meridional winds, and electric field drifts. Others authors focussed their attention on single or few events [*Nicolls et al*., 2006; *Liu et al*., 2008a, b; *Zhao et al*., 2008].

In order to explain some nighttime *Nm*F2 enhancements recorded at equatorial latitudes, *Nicolls et al*. [2006] showed that near the magnetic equator, the uplifts are generally not the result of a zonal electric field reversal, but rather due to a decreasing westward electric field, caused by a change in the wind system related to the midnight pressure bulge. Nevertheless, they asserted that the interpretation of the nighttime electron density increases in terms of the reverse fountain effect is not satisfactory and, as an alternative they suggested a horizontal gradient in the meridional plasma flux.

Liu et al. [2008a, b] investigated strong pre-storm enhancements at low latitudes in the equatorial ionospheric anomaly, and they ascribed them to an enhanced equatorial eastward zonal electric field. They found that the pre-storm enhancements are simultaneously presented in *fo*F2 and TEC, tend to occur with peaks around the equatorial anomaly crests, and are not characterized by a corresponding change of *hm*F2 at latitudes poleward of the northern crest.

Zhao et al. [2008] investigated an anomalous enhancement during a geomagnetically quiet day after local sunset where the low latitude value of *Nm*F2 was observed to increase by 200% compared to the 27-day median value. Although not in agreement with the prediction of *Scherliess and Fejer* [1997] and *Nicolls et al*. [2006], they attributed this phenomenon mainly to an increase in the eastward zonal electric field.

This work investigates a large electron density nighttime enhancement that occurred on the 6th of March 2010 over a wide region of South America, below the southern crest of the equatorial anomaly, during low solar activity and quiet geomagnetic conditions. It is important to note that the present

investigation focuses on a very unusual event which we called “impulsive enhancement” because a sudden increase in electron density was immediately followed by an equally rapid recovery phase. In addition, this impulsive enhancement corresponded with a pronounced compression of the ionosphere, which is very distinctive.

To the best of the authors’ knowledge, this is the first time that such an impulsive phenomenon has been observed almost simultaneously by different low latitude ionosondes widely distributed in space.

The present analysis, which is based on ionosonde data, GPS measurements, and equatorial zonal electric field data recorded by the Communications/Navigation Outage Forecasting System (C/NOFS) satellite, developed by the Air Force Research Laboratory Space Vehicles Directorate, suggests that an enhanced fountain effect and plasma diffusion from the plasmasphere might not be solely responsible for the observed sudden increase in the electron density.

The analyses of the isoheight and isofrequency ionosonde plots suggest that travelling ionospheric disturbances (TIDs) might have played a significant role.

2. Data Sets

The analysis was based on data recorded from five ionosondes and twelve GPS receivers located in South America (see Table 1 for the corresponding locations). The International Geomagnetic Reference Field 11 [*Finlay et al*., 2010] was used to calculate the geomagnetic latitude of the ionosonde and the GPS receivers’ stations.

In order to detect the peculiar *fo*F2 nighttime impulsive enhancement that occurred on the 6th of March 2010, a period of low solar activity (R_{12}=15), reference was made to the autoscaling visualization feature of the electronic Space Weather upper atmosphere database (eSWua; http://www.eswua.ingv.it/) [*Romano et al*., 2008], simply by checking the daily *fo*F2 plots computed from August 2007 to July 2010 on the basis of the *fo*F2 values produced automatically as output by

Autoscala [*Pezzopane and Scotto*, 2007] from the ionograms recorded at Tucumán (26.9° S, 65.4° W, magnetic latitude 16.8° S), Argentina. Without this autoscaling visualization feature of eSWua, it would have been impossible to notice the impulsive peculiarity of the event under study, which is the only one occurring during quiet geomagnetic conditions since August 2007, a period during which an AIS-INGV (Advanced Ionospheric Sounder-Istituto Nazionale di Geofisica e Vulcanologia) ionosonde was installed at the new ionospheric station of Tucumán [*Pezzopane et al*., 2007].

The ionograms considered for the present study were those recorded in March 2010 at Jicamarca (12.0° S, 76.8° W, magnetic latitude 2.0° S), Peru, Sao Luis (hereafter referred to as SL; 2.6° S, 44.2° W, magnetic latitude 6.2° N), Cachoeira Paulista (hereafter referred to as CP; 22.4° S, 44.6° W, magnetic latitude 13.4° S), São José dos Campos (hereafter referred to as SJC; 23.2° S, 45.9° W, magnetic latitude 14.1° S), Brazil, and Tucumán. An attempt was also made to analyze equatorial ionograms from Fortaleza (3.8° S, 38.0° W, magnetic latitude 4.5° S) and Palmas (10.2° S, 48.2° W, magnetic latitude 1.0° S), Brazil, but unfortunately on the 6th of March 2010 most of the ionograms recorded at these stations were characterized by strong spread-F phenomena and it was impossible to derive reliable and continuous *fo*F2 values in the hours of interest.

The ionospheric station at SJC is equipped with a Canadian Advanced Digital Ionosonde (CADI) [*MacDougall et al*., 1993] and in March 2010 the sounding repetition rate and sweeping frequency range were set to 5 minutes and from 1 MHz to 20 MHz respectively. The ionospheric stations at Jicamarca, SL and CP are equipped with a digisonde [*Bibl and Reinisch*, 1978]. In March 2010 the sounding repetition rate of the Jicamarca, SL, and CP digisondes was set to 15, 10 and 7 minutes respectively. The sweeping frequency range at Jicamarca was variably set from 1 to 15 MHz and from 1 to 12 MHz, while at SL and CP was set from 1 MHz to 14 MHz. The data were downloaded from the Global Ionospheric Radio Observatory web portal [*Reinisch et al*., 2004]. In March 2010 the sounding

repetition rate and the sweeping frequency range of the AIS-INGV ionosonde installed at Tucumán were set to 15 minutes and from 1.5 MHz to 15 MHz respectively.

The GPS data were obtained from the International Global Navigation Satellite System Service (IGS) database [*Dow et al*., 2009]. Twelve receivers (see Table 1) were used to compute TEC values in a region extending in latitude from 0° S to 45° S and in longitude from 50° W to 80° W.

The level of geomagnetic activity characterizing the period under investigation is indicated by the 3 hourly-*Kp*, *Dst*, and *AE* indices, which were downloaded from the World Data Center for Geomagnetism, Kyoto, Japan from the web site http://wdc.kugi.kyoto-u.ac.jp/. *AE*, with hourly resolution, is used as an indicator of substorm activity, *Kp* describes geomagnetic conditions at mid latitudes, and *Dst*, strictly connected with the ring current state, describes geomagnetic conditions at low latitudes.

Data were not available from the Jicamarca Unattended Long-term Investigations of the Ionosphere and Atmosphere (JULIA) radar installed in Jicamarca. This would have been useful to evaluate the electric field direction and amplitude, and so the equatorial zonal electric field data recorded on the 6th of March 2010 by the C/NOFS satellite was used instead.

3. Results

Figure 1 shows respectively the 3 hourly-*Kp*, *Dst*, and *AE* indices recorded from the 1st to the 8th of March 2010. *Dst* never goes under -30 nT and according to the storm classification made by *Gonzalez et al*. [1994] these disturbances are too small to be considered as storms. *Kp* is noticeably low reaching a maximum value of 3 only in four periods. *AE* hourly values are in general quite low and the few high values never exceed 500 nT, this kind of trend being rather common. *AE* values well above 500 nT are necessary to trigger intense substorms, causing serious ionospheric plasma modification at mid and low latitudes [*Akasofu*, 1970; *Prölss*, 1993]. This observation is further supported by the unperturbed *fo*F2

plots shown in Figure 2 and obtained at the mid-high latitude ionospheric station of Comandante Ferraz (EACF; 62.1° S, 58.4° W, magnetic latitude 52.2° S), Brazil, equipped with a CADI, on the 5th, 6th, and 7th of March 2010.

In order to investigate the spatial extent of the unusual nighttime impulsive *fo*F2 enhancement detected at Tucumán, Figures 3a-e show the *fo*F2 plots obtained at Jicamarca, SL, CP, SJC, and Tucumán on the 6th of March 2010 after manually validating the corresponding ionograms according to the International Union of Radio Science (URSI) standard [*Wakai et al*., 1987]. Unfortunately, on the 6th of March 2010 at Jicamarca from 04:00 to 05:30 Universal Time (UT) and at SJC from 02:00 to 05:30 UT the ionograms were characterized by spread-F phenomena and it was impossible to obtain a value for *fo*F2. The ionograms from Jicamarca, SL and CP were validated using the SAO explorer programme developed by the University of Massachusetts, Lowell, the ionograms from SJC were validated using the Digital Ionosonde Data Analysis system developed by the Universidade do Vale do Paraíba, and the ionograms from Tucumán were validated using the Interpre software developed by *Pezzopane* [2004]. In particular, for SJC and Tucumán all the ionograms recorded in March 2010 were considered and, once the validated *fo*F2 values had been obtained, the corresponding mean (green curve in Figures 3d, 3e) and standard deviation (red and black curves in Figures 3d, 3e represent respectively the mean ± the standard deviation) were calculated.

In Figure 3e, a significant and rapid (less than two hours) increase in *fo*F2 beginning at about 05:00 UT is evident at Tucumán (LT = UT - 4). The phenomenon is extremely impulsive, and the bell-shaped trend of the *fo*F2 plot is very narrow, because after reaching a peak, the *fo*F2 falls to very low values and the decrease phase is even more rapid (about one hour) than the increase phase. Even though less pronounced, Figures 3c-d show that the same phenomenon also occurs at CP (LT = UT - 3) and SJC (LT = UT - 3). The *fo*F2 peak enhancement is about 100% of the mean value at Tucumán, while at SJC it is about 55% of the mean value. Moreover, given that the *fo*F2 plots obtained at Jicamarca and SL do

not exhibit any impulsive enhancement, Figure 3 also highlights how the event was confined around the southern anomaly crest.

Figure 4 shows the same as Figure 3 but for the virtual height of the base of the F layer (*h*'F). The striking feature that emerges by comparing Figures 3c-e and 4c-e, is that at CP, SJC, and Tucumán when *fo*F2 undergoes impulsive enhancement and reaches its maximum value, the ionosphere is strongly compressed. This suggests that a combined secondary fountain effect and downward plasma diffusion from the plasmasphere cannot be considered the only agents responsible for the event, and that something like a TID might have played a substantial role (*Lu et al*., 2001). Again, at Jicamarca and SL the *h*'F trend does not exhibit any significant feature.

In order to look for the possible presence of TIDs caused by gravity wave (GW) propagation, the ionogram traces recorded at Tucumán on the 6th of March 2010 from 00:00 to 10:00 UT were manually digitized, obtaining an electron density profile (*N*, *h*') for each ionogram, where *N* is the electron density and *h*' is the virtual height of reflection. Then inversion from the profile (*N*, *h*') to the profile (*N*, *h*), where *h* is the real height of reflection, was performed using the POLAN inversion technique [*Titheridge*, 1988]. From the profiles (*N*, *h*) isoheight curves *N*(*h*=const=170, 180, 190, 200, 210, 220, 230, 240, 250, 260, 270, 280, 290, 300 km) were obtained and plotted in Figure 5a. Figure 5b shows that from 06:00 to 08:00 UT (02:00 to 04:00 LT) maximum *N* variations occur first at 220 km and then at lower heights, showing a downward phase shift which is characteristic of GW propagation in the ionospheric F region [*Hines*, 1960]. Using isoheight curves shown in Figure 5, it is possible to estimate the GW period *T*. In fact, even though Figure 5 does not show neither two consecutive peaks nor two consecutive valleys, focusing the attention on isoheight curves *N*(*h*=170 km) and *N*(*h*=180 km), the distance between the peak and the valley, corresponding to *T*/2, is quite definite and equal to 45 minutes (*T*=90 minutes). The vertical phase velocity v_z is calculated using the peak of two consecutive heights, as illustrated in Figure 5b, and a value of $v_z \approx 11$m/s is found; the vertical

wavelength $\lambda_z = v_z T \approx 60$km is then obtained. These values of T, v_z, and λ_z are consistent with the analysis performed by *Klausner et al*. [2009] using a digisonde at SJC during low solar activity. The corresponding horizontal wavelength (λ_h) can be determined using a relationship between λ_h and λ_z given by *Hines* [1960], namely, $\omega^2\lambda_h^2 \approx (\omega_g^2 - \omega^2)\lambda_z^2$, where ω_g is the Brunt-Väisälä frequency, which was taken as $2\pi/14$ min^{-1} [*Abdu et al*., 1982], and $\omega = 2\pi/T$ is the wave angular frequency. The horizontal wavelength comes out to be $\lambda_h \approx 380$ km, which is a value consistent with a medium scale TID (MSTID).

Electron density profiles obtained at Tucumán on the 6th of March 2010 at 05:00, 06:30, 08:15, and 08:30 UT using the POLAN inversion technique are shown in Figure 6. This figure clearly illustrates the compression and the expansion phases characterizing the F layer, and also how the impulsive enhancement of *fo*F2 is associated with the compression phase.

Figure 7 shows the virtual height variations at six fixed frequencies 3, 4, 5, 6, 7, and 8 MHz recorded at SJC on the 6th of March 2010 from 00:00 to 08:00 UT. From 06:00 to 07:00 UT at minima the downward phase shift characteristic of GW propagation is quite clear, on the contrary from 02:00 to 04:00 UT at maxima due to spread-F phenomena is quite blurred. As a consequence, in this case it is not reliable to perform an estimation of the GW parameters in the same way as done for Tucumán.

In order to establish deeper analysis of the behaviour of the ionosphere from the geomagnetic equator towards the southern crest of the anomaly, Figure 8 illustrates the time sequence of two-dimensional maps of vertical TEC (vTEC) over South America on the 6th of March 2010 from 04:30 to 07:00 UT with a 10 minute interval, over an area extending from 0° S to 45° S in latitude and from 50° W to 80° W in longitude. This region was considered because within it the GPS receivers, with data downloadable from IGS, are sufficiently dense to guarantee good quality of the two-dimensional computation of vTEC. In order to generate these figures, twelve GPS receivers (see Table 1) were included. The slant TEC (sTEC) values, affected by an offset Ω_{Arc}, constant for each "phase-

connected" arc of data [*Mannucci et al*., 1998], were obtained for each receiver from the frequency differenced phase delay S (where S=sTEC+Ω_{Arc}) computed from the RINEX files. In order to avoid problems with the levelling procedure, instead of levelling the slants to differential pseudoranges, offsets were directly estimated, receiver by receiver, using a multi-day thin shell (400 km) solution [*Ciraolo et al*., 2007]. After estimating the offsets, the resulting sTEC values (sTEC=S-Ω_{Arc}) were then converted to vTEC values at the ionospheric pierce point using the well known mapping function vTEC=sTEC·cosχ, where χ is the angle formed by the satellite-receiver line of sight and the normal at the thin shell. These vTEC values are then used to generate the two-dimensional maps shown in Figure 8 applying a polynomial Kriging interpolation (3rd order in latitude and longitude displacement). In Figure 8 it is worth noting that some receivers listed in Table 1 are outside the region considered but their inclusion is useful to ensure a reliable interpolation over the area under investigation.

Figure 8 shows that from 04:30 to 05:00 UT the electron density is larger around the magnetic equator, and that from 05:00 to 07:00 UT a reversal is observed. The most interesting feature is that the reversal is confined in a region over Tucumán between about 20° S and 28° S in latitude, and between 60° W and 70° W in longitude, where a structure of enhanced plasma starts forming at about 05:00 UT and vanishes at about 07:00 UT.

In order to investigate the nature of the distribution of ionization in more detail, we used the vTEC calculated over Tucumán to compute the corresponding slab thickness (vTEC/NmF2) for the 6th of March 2010. This represents the equivalent thickness of the ionosphere having a constant uniform density equal to the F2 layer peak electron density. The result is shown in Figure 9, from which it is clear that the variations of this parameter during that night were unusual because after dropping to values less than 100 km at about 07:00 UT, it rose to values greater than 1000 km at about 09:00 UT, and then dropped again to 200 km at about 11:00 UT.

Finally, Figure 10 shows the zonal electric field recorded on the 6th of March 2010 by the C/NOFS satellite, over an area extending from 12.3° N to 2.8° S in latitude, and from 40° W to 90° W in longitude, in an altitude range from 530 to 818 km, from 00:00 to 05:00 LT averaging on ten-minute bins. A pronounced decrease of the westward electric field is evident from 00.30 to 01:30 LT.

4. Discussion

Using ground based measurements it was shown that on the 6th of March 2010 the ionosphere suffered a significant nighttime modification in the South American region. The main features of this event can be summarized as follows: (1) anomalous and impulsive postmidnight enhancement of *fo*F2 recorded at some ionospheric stations widely distributed in space and located below the southern crest of the equatorial anomaly; (2) anomalous structure of enhanced TEC over a restricted region affected by the phenomenon; (3) strong compression of the ionosphere; (4) magnetic activity relatively low.

The postmidnight time of occurrence of this enhancement along with its very short duration and the associated compression of the ionosphere makes this event very distinctive. Also, the fact that the nighttime enhancement investigated in this paper occurred during geomagnetically quiet conditions is quite significant because recently *Pavlov and Pavlova* [2007] found that this kind of phenomena occur mainly during geomagnetically disturbed conditions.

Initially, this phenomenon was thought to be caused by the passage of a plasma blob, with a local increase in plasma density [*Oya et al*., 1986; *Watanabe et al*., 1986]. However, we believe that this cannot be correct based on two reasons. First, the impulsive enhancement under study is visible at different ionospheric stations quite remote from each other, and secondly, the creation of a blob is related to an upward shift of the bottomside F region [*Kil et al*., 2011], whereas in this case the *fo*F2 enhancement and the F region height shift are anticorrelated.

Postsunset enhancements are known to be caused by the prereversal increase of the equatorial fountain [*Woodman*, 1970], which can raise the F region to altitudes of lower chemical loss, and the subsequent diffusion of ionization along the magnetic field lines causes the nighttime plasma enhancements at latitudes around the equatorial anomaly regions [*Anderson and Klobuchar*, 1983].

On the contrary, the mechanisms responsible for the postmidnight enhancements is yet to be clearly clarified. *Bailey et al*. [1991], *Richards et al*. [2000a], and *Pavlov and Pavlova* [2005] agreed on the explanation that large downward plasma fluxes are responsible for postmidnight enhancements. *Mikhailov et al*. [2000a, b] proposed that the observed postmidnight *Nm*F2 enhancements were due to the uplifting of the F2 layer by the equatorward thermospheric winds, along with the observed nighttime plasmaspheric fluxes into the F2 region.

However, in each location, the relative change of *h*'F will modify the loss rate of the ions and hence act as one of the important factors that can affect the nighttime *Nm*F2 enhancements [*Sastri*, 1998], and several authors [*Su et al*., 1994; *Farelo et al*., 2002; *Nicolls et al*., 2006] agreed that postmidnight enhancements are mainly related to an uplift of the F layer. Nevertheless, this explanation may not be true for the event investigated here, because the impulsive enhancement of *fo*F2 and TEC highlighted by Figures 3c-e and 8 was associated with a definite compression of the F layer, as shown by Figures 4c-e, 6, and 9.

Compared to other similar events [e.g., *Nicolls et al*., 2006; *Zhao et al*., 2008], the features of this *fo*F2 nighttime enhancement are clearly different. Compared to the events described by *Nicolls et al*. [2006], the event discussed in this paper is in fact characterized by a larger amplitude and a much shorter duration. The anomalous enhancement investigated by *Zhao et al*. [2008] was instead comparable in terms of amplitude, but had a duration of more than six hours, much longer than the duration of the impulsive event investigated here.

The impulsive event in question does not even fall within the range of the study conducted by *Balan and Rao* [1987]. At equatorial anomaly latitudes, under solar minimum conditions, these authors found that the highest values of the mean peak amplitude were associated with a mean half-amplitude duration of 3 hours and that lowest values of the mean peak amplitude were associated with a mean half-amplitude duration of 1.5 hours.

Concerning the local time of occurrence characterizing the impulsive event under study, this was consistent with the findings of *Su et al*. [1994] and *Farelo et al*. [2002] who showed that there are major peaks in the frequency of occurrence at around 20:00 LT for postsunset enhancements and at 01:00-02:00 LT for postmidnight enhancements, and that most enhancements occur around, or after, midnight during the solar minimum. However, they again found that the mean half-amplitude duration was about 2.5-3 hours and that postmidnight enhancements become stronger with increasing solar activity, which contrasts with the features of the impulsive event investigated by the present study.

Liu et al. [2008a, b] investigating pre-storm enhancements showed that these tended to occur with peaks around latitudes of the southern and northern equatorial anomaly crests, and in virtue of this they suggested they were probably due to an enhanced equatorial eastward zonal electric field. The event described in this study seems to be very similar to those illustrated by *Liu et al*. [2008a, b], both because the enhancement, as shown by Figures 3c-e and 8, was confined around the southern anomaly crest and also because, as shown by Figure 10, the westward zonal electric field decreases noticeably from 00:30 to 01:30 LT. The latter agrees with *Nicolls et al*. [2006] who asserted that a nighttime secondary effect is not caused only by a reversal of the zonal electric field but might also be due to a decreasing westward electric field, which in practice would correspond to the enhancement of the eastward electric field proposed by *Liu et al*. [2008a, b]. Nevertheless, *Liu et al*. [2008a, b] found that at latitudes 5°-8° north of the northern crest the pre-storm enhancements were not characterized by a corresponding change of *hm*F2. On the contrary, the most intriguing feature of the observed

phenomenon emerging from the overall examination of Figures 3c-e, 4c-e, 6, 8 and 9 is that the impulsive increase of electron density is associated with a significant compression of the ionosphere.

In order to explain this anticorrelation, *Lu et al*. [2001] illustrated that when the meridional wind is the dominant influence on the F2 layer, the positive/negative vertical wind shear caused by upward GW propagation can compress/expand the layer, leading to such an anticorrelation. Figure 5 and partly also Figure 7 confirm what *Lu et al*. [2001] suggested, and highlight that GW propagation might actually play a significant role in impulsive enhancements characterized by very large amplitude and very short duration, like the one investigated in this work.

TIDs are generally considered as plasma manifestations of GWs propagating in the ionosphere [*Hines*, 1960]. Electrodynamic processes, like Perkins instability, and some sort of mechanism, for example GW propagation, are required for the generation of MSTIDs, which have horizontal wavelength between 50 and 500 km, periods of 1 to 2 hours, and propagate with a velocity between 50 and 170 m/s [*Shiokawa et al*., 2003]. The horizontal wavelength of 380 km estimated from Figure 5 is consistent with a MSTID.

Recently, two-dimensional mapping techniques using GPS receiver networks were demonstrated to be a very powerful tool for investigating TEC latitudinal distributions [*Valladares et al*., 2001], eastward motion of the background ionosphere [*Valladares et al*., 2004], and propagation of MSTIDs [*Kotake et al*., 2007; *Tsugawa et al*., 2007].

Using the Portable Ionospheric CAmera and Small-Scale Observatory (PICASSO) located at La Serena (30.2° S, 70.8° W, magnetic latitude 16.7° S) in Chile, *Makela et al*. [2010] found evidence of MSTIDs approaching the geomagnetic equator over western South America. These structures are elongated from northwest to southeast in the northern hemisphere and from southwest to northeast in the southern hemisphere, they propagate westward and towards the equator perpendicularly to their long dimension. It should be noted that, before the work by *Makela et al*. [2010], MSTIDs were

thought to occur in the mid latitude ionosphere and not at magnetic latitudes equatorward of the equatorial anomalies.

In the two-dimensional TEC maps computed by the present authors (Figure 8) no feature associated with MSTID propagation is visible. In order to point out MSTID signatures, methods like for instance the detrending one used by *Tsugawa et al*. [2007] are more appropriate. Nevertheless, with regard to this we have to stress the fact that the density of GPS receivers in the South America is quite low and not sufficient to perform analyses like the one done in the North America by *Tsugawa et al*. [2007] who exploited a dense network of more than 1400 GPS receivers. Nonetheless, in Figure 8 it can be seen that from 04:30 to 05:00 UT the electron density was larger around the magnetic equator, but then from 05:00 UT to 07:00 UT a reversal is observed, in a restricted region over Tucumán between about 20° S and 28° S in latitude, and between 60° W and 70° W in longitude. The increase of electron density around the magnetic equator from 04:30 to 05:00 UT is likely due to a large reverse fountain according to the mechanism proposed by *Balan and Bailey* [2005]. Typically the reverse fountain starts at about 20:00 LT when the **E**x**B** drift turns downward. The ionization, which has been in the topside F region around the equator, is pushed downward across the magnetic field lines by the downward **E**x**B** drift and thereby creates a low plasma pressure region in the topside ionosphere. To fill this low-pressure region, plasma flows towards the equator from both sides. This plasma is again pushed downward across the magnetic field lines. The nighttime TEC increases are then strongest at the equator and become weaker with increasing latitude. Hence, looking at Figure 8, the increase of electron density characterizing the magnetic equator from 04:30 to 05:00 UT is likely due to a large reverse fountain starting well after 20:00 LT. This is also supported by what shown by Figure 10 where it is possible to see that at about 00:30 LT the westward electric field increases very much. From 05:00 to 07:00 UT, the TEC value near the magnetic equator diminished while at the southern crest increased, indicating a recharging of the fountain effect. The recharging of the fountain effect, according to what

evidenced by *Nicolls et al*. [2006], is supported by the fact that westward (eastward) zonal electric field measured by the C/NOFS satellite strongly decreases (increases) (see Figure 10). However, the correspondent anomaly is slight and restricted in a little region over Tucumán. The TEC enhancement is then different with respect to the *fo*F2 enhancement which is instead widely distributed in space.

It is important to note that the nighttime variations of TEC and *fo*F2 are not necessarily the same because variations in TEC depend not only on changes in *fo*F2 but also on the density of the nighttime plasmasphere and topside ionosphere [*Maruyama et al*., 2004]. *Maruyama et al*. [2004] found prominent quantitative dissimilarities in comparing the amplitudes of the positive and negative perturbations in TEC and *fo*F2 at lower geomagnetic latitudes. Generally, the daytime correlation between changes in TEC and the critical frequency *fo*F2 at low geomagnetic latitudes is higher than the nighttime correlation [*Houminer and Soicher*, 1996].

Besides, the difference between what is shown by Figure 3 and by Figure 8 might be due to a greater recharging of the electric field characterizing the longitudinal sector around Tucumán rather than the longitudinal sectors east of Tucumán. This is somehow confirmed by Figure 3c-e where the *fo*F2 impulsive enhancement is by far greater at Tucumán than at the ionospheric stations east of Tucumán.

Moreover, a careful examination of Figures 3c-e and 4c-e reveals that the phenomenon was observed at CP and SJC about one hour prior to Tucumán. This time delay could be caused both by the different effect that the fountain effect can produce at different latitudes, and, as suggested by *Nicolls et al*. [2006], by electron fluxes coming from the plasmasphere and moving westward.

Furthermore, it is important to stress again that an increase of electron density associated with a compression of the ionosphere implies that, besides considering an enhanced fountain effect and a plasma diffusion from the plasmaphere, also TIDs should be taken into account to explain the phenomenon.

According to this and to the evidence given by *Makela et al*. [2010] that MSTIDs can propagate also equatorward of the equatorial anomalies, Figure 11 illustrates the wave front of a MSTID propagating in the northwest direction, that is coherent with the fact that the *fo*F2 enhancement is observed before at CP and SJC and approximately one hour later at Tucumán, assuming for the MSTID a phase velocity of about 80 m/s, which is consistent with the T and the λ_h previously found, and a distance between Tucumán and SJC along the propagation direction of about 400 km.

The amplification of the phenomenon at Tucumán, as seen both by the *fo*F2 plots of Figure 3c-e and by the two-dimensional TEC maps of Figure 8, could be due to the fact that the longitudinally dependent **E**x**B** upward drift and the westward electron fluxes coming from the plasmasphere progressively add up to the northwestward MSTID caused by GW propagation.

5. Summary

Nighttime electron density enhancements are called "anomalous enhancements", because the solar UV radiation, which is the major source of ionization, is absent during the night.

In this paper, electron density was shown to undergo an anomalous postmidnight enhancement at the southern anomaly crest during quiet geomagnetic conditions and low solar activity, referred to as an "impulsive enhancement". The event investigated was in fact very particular because, besides being observed almost simultaneously at different ionospheric stations widely distributed in space, it was characterized by its large amplitude and extremely short duration, which clearly distinguishes it from single events studied by other authors [*Liu et al*., 2008a, b; *Nicolls et al*., 2006; *Zhao et al*., 2008].

In reality, the confinement around the southern anomaly makes the event described in this study similar to those illustrated by *Liu et al*. [2008a, b]. However, contrary to what was found by *Liu et al*. [2008a, b], another feature that makes this event unusual was a pronounced simultaneous compression undergone by the ionosphere, which is also contrary to the more common mechanism that associates

postmidnight enhancements with an uplift of the F layer [e.g., *Su et al*., 1994, *Sastri*, 1998; *Farelo et al*., 2002, *Nicolls et al*., 2006].

Consequently, these nighttime enhancement features cannot be attributed entirely to an enhanced fountain effect or plasma diffusion from the plasmasphere, as highlighted by several authors [*Bailey et al*., 1991; *Mikhailov et al*., 2000a,b; *Richards et al*., 2000a, b; *Pavlov and Pavlova*, 2005; *Nicolls et al*., 2006; *Liu et al*., 2008a, b].

Moreover, even though more pronounced at Tucumán, the *fo*F2 enhancement is widely distributed in space, while on the contrary the TEC enhancement appears restricted in a region around Tucumán.

The present study suggests that the three probable physical processes that could be (jointly) responsible for the observed features are:

1) a greater recharging of the fountain effect due to a strong decrease of the equatorial zonal westward electric field, this being larger in the longitudinal sector around Tucumán rather than in the longitudinal sectors east of Tucumán;
2) westward electron fluxes coming from the plasmasphere;
3) a MSTID propagating in the southern hemisphere towards the equator in the northwest direction.

Acknowledgements

The authors gratefully acknowledge the three reviewers for their helpful comments and suggestions.

References

Abdu, M. A., I. S. Batista, I. J. Kantor, and J. H. A. Sobral (1982), Gravity wave induced ionization layers in the night F-region over Cachoeira Paulista (22°S, 45°W), *J. Atmos. Terr. Phys.*, 44, 759–767.

Akala, A. O., A. B. Adeloye, and E. O. Somoye (2010), Ionospheric foF2 variability over the Southeast Asian sector, *J. Geophys. Res.*, 115, A09329, doi:10.1029/2010JA015250.

Akasofu, S. I. (1970), Diagnostics of magnetosphere using geomagnetic, auroral and airglow phenomena, *Ann. Geophys.*, 26, 443–457.

Anderson, D. N., and J. A. Klobuchar (1983), Modelling the total electron content observations above Ascension Island, *J. Geophys. Res.*, 88, A10, doi:10.1029/JA088iA10p08020.

Bailey, G. J., R. Sellek, and N. Balan (1991), The effect of interhemispheric coupling on nighttime enhancements in ionospheric total electron content during winter at solar minimum, *Ann. Geophys.*, 9, 734–747.

Balan, N., and P. B. Rao (1987), Latitudinal variations of nighttime enhancements in total electron content, *J. Geophys. Res.*, 92, A4, doi:10.1029/JA092iA04p03436.

Balan, N., G. J. Bailey, and B. B. Nair (1991), Solar and magnetic activity effects on the latitudinal variations of nighttime TEC enhancement, *Ann. Geophys.*, 9, 60–69.

Balan, N., G. J. Bailey, B. B. Nair, and J. E. Titheriedge (1994), Nighttime enhancements in ionospheric electron content in the northern and southern ionosphere, *J. Atmos. Sol. Terr. Phys.*, 56, 67–69.

Balan, N., and G. J. Bailey (1995), Equatorial plasma fountain and its effects: Possibility of an additional layer, *J. Geophys. Res.*, 100, A11, doi:10.1029/95JA01555.

Bibl, K., and B. W. Reinisch (1978), The universal digital ionosonde, *Radio Sci.*, 13, 519–530.

Borries, C., and P. Hoffmann (2010), Characteristics of F2 layer planetary wave–type oscillations in northern middle and high latitudes during 2002 to 2008, *J. Geophys. Res.*, 115, A00G10, doi:10.1029/2010JA015456.

Buresova, D., and J. Laštovička (2008), Pre-storm electron density enhancements at middle latitudes, *J. Atmos. Terr. Phys.*, 70, 1848-1855, doi:10.1016/j.jastp.2008.01.014.

Chen, Y., and L. Liu (2010), Further study on the solar activity variation of daytime NmF2, *J. Geophys. Res.*, 115, A12337, doi:10.1029/2010JA015847.

Ciraolo, L., F. Azpilicueta, C. Brunini, A. Meza, and S. M. Radicella (2007), Calibration errors on experimental slant total electron content (TEC) determined with GPS, *J. Geodesy*, 81, 111-120, doi:10.1007/s00190-006-0093-1.

David, M., and Jan J. Sojka (2010), Single-day dayside enhancements over Europe: A survey of a half-century of ionosonde data, *J. Geophys. Res.*, 115, A12311, doi:10.1029/2010JA015711.

Depueva, A. K., A. V. Mikhailov, and V. K. Depuev (2005), Quiet time F2 layer disturbances at geomagnetic equator, *Int. J. Geomagn. Aeron.*, 5, GI3001, doi:10.1029/2004GI000071.

Dow, J. M., R. E. Neilan, and C. Rizos (2009), The International GNSS Service in a changing landscape of Global Navigation Satellite Systems, *J. Geodesy*, 83, 191–198, doi:1007/s00190-008-0300-3.

Ezquer, R. G., M. Mosert, R. Corbella, M. Erazù, S. M. Radicella, M. Cabrera, L. de la Zerda (2004), Day-to-day variability of ionospheric characteristics in the American sector, *Adv. Space Res.*, 34, 1887-1893, doi:10.1016/j.asr.2004.03.016.

Farelo, A. F., M. Herraiz, and A.V. Mikhailov (2002), Global morphology of nighttime NmF2 enhancements, *Ann. Geophys.*, 20, 1795-1806.

Finlay et al. (2010), International Geomagnetic Reference Field: the eleventh generation, *Geophys. J. Int.*, 183, 1216-1230, doi:10.1111/j.1365-246X.2010.04804.x.

Gonzalez, W. D., J. A. Joselyn, Y. Kamide, W. Krochl, G. Rostoker, B. T. Tsurutani, and V. M. Vasyliunas (1994), What is a geomagnetic storm?, *J. Geophys. Res.*, 99, 5771-5792.

Hall, C. M., K. Rypdal, and M. Rypdal (2011), The E region at 69°N, 19°E: Trends, significances, and detectability, *J. Geophys. Res.*, 116, A05309, doi:10.1029/2011JA016431.

He, M., L. Liu, W. Wan, and B. Zhao (2011), A study on the nighttime midlatitude ionospheric trough, *J. Geophys. Res.*, 116, A05315, doi:10.1029/2010JA016252.

Hines, C. O. (1960), Internal atmospheric gravity waves at ionospheric heights, *Can. J. Phys.*, 38, 1441–1481.

Houminer, Z., and H. Soicher (1996), Improved short-term predictions of foF2 using GPS time delay measurements, *Radio Sci.*, 31, 5, doi:10.1029/96RS01965.

Janve, A. V., R. K. Rai, M. R. Deshpande, R. C. Rastogi, A. R. Jain, M. Singh, and H. S. Gurm (1979), On the nighttime enhancements in ionospheric total content at low latitudes, *Ann. Geophys.*, 35, 159–165.

Kil, H., H.-S. Choi, R. A. Heelis, L. J. Paxton, W. R. Coley, and E. S. Miller (2011), Onset conditions of bubbles and blobs: A case study, *Geophys. Res. Lett.*, 38, L06101, doi:10.129/2011GL046885.

Klausner, V., P. R. Fagundes, Y. Sahai, C. M. Wrasse, V. G. Pillat, and F. Becker-Guedes (2009), Observations of GW/TID oscillations in the F2 layer at low latitude during high and low solar activity, geomagnetic quiet and disturbed periods, *J. Geophys. Res.*, 114, A02313, doi:10.1029/2008JA013448.

Kotake, N, Y. Otsuka, T. Ogawa, T. Tsugawa, and A. Saito (2007), Statistical study of medium-scale travelling ionospheric disturbances observed with the GPS networks in Southern California, *Earth Planets Space*, 59, 95-102.

Kouris, S. S., and D. N. Fotiadis (2002), Ionospheric variability: A comparative statistical study, *Adv. Space Res*., 29, 977-985, doi:10.1016/S0273-1177(02)00045-5.

Lee, W. K., H. Kil, Y.-S. Kwak, Q. Wu, S. Cho, and J. U. Park (2011), The winter anomaly in the middle-latitude F region during the solar minimum period observed by the Constellation Observing System for Meteorology, Ionosphere, and Climate, *J. Geophys. Res*., 116, A02302, doi:10.1029/2010JA015815.

Lin, C. H., C. H. Liu, J. Y. Liu, C. H. Chen, A. G. Burns, and W. Wang (2010), Midlatitude summer nighttime anomaly of the ionospheric electron density observed by FORMOSAT□3/COSMIC, *J. Geophys. Res*., 115, A03308, doi:10.1029/2009JA014084.

Liu, G., T. J. Immel, S. L. England, K. K. Kumar, and G. Ramkumar (2010), Temporal modulations of the longitudinal structure in F2 peak height in the equatorial ionosphere as observed by COSMIC, *J. Geophys. Res*., 115, A04303, doi:10.1029/2009JA014829.

Liu, L., Y. Chen, H. Le, V. I. Kurkin, N. M. Polekh, and C.-C. Lee (2011), The ionosphere under extremely prolonged low solar activity, *J. Geophys. Res*., 116, A04320, doi:10.1029/2010JA016296.

Liu, L. , B. Zhao, W. Wan, B. Ning, M.-L. Zhang, and M. He (2009), Seasonal variations of the ionospheric electron densities retrieved from Constellation Observing System for Meteorology, Ionosphere, and Climate mission radio occultation measurements, *J. Geophys. Res.*, 114, A02032, doi:10.1029/2008JA013819.

Liu, L., W. Wan, M.-L. Zhang, B. Zhao, and B. Ning (2008), Prestorm enhancements in NmF2 and total electron content at low latitudes, *J. Geophys. Res.*, 113, A02311, doi:10.1029/2007JA012832.

Liu, L., W. Wan, M.-L. Zhang, and B. Zhao (2008), Case study on total electron content enhancements at low latitudes during low geomagnetic activities before the storms, *Ann. Geophys.*, 26, 893–903.

Lois, L., H. Peres, B. Lazo, N. Jakowski, and R. Landrock (1990), Nighttime enhancement of the F2-layer ionization over Havan-Cuba: a relationship with solar activty, *Int. J. Geomagn. Aeron.*, 30, 76-82.

Lu, G., A. D. Richmond, R. G. Roble, and B. A. Emery (2001), Coexistence of ionospheric positive and negative storm phase under northern winter conditions: A case study, *J. Geophys. Res.*, 106, A11, doi:10.1029/2001JA000003.

Luan, X., W. Wang, A. Burns, S. C. Solomon, and J. Lei (2008), Midlatitude nighttime enhancement in F region electron density from global COSMIC measurements under solar minimum winter condition, *J. Geophys. Res.*, 113, A09319, doi:10.1029/2008JA013063.

MacDougall, J. W., I. F. Grant, and X. Shen (1993), The Canadian Advanced Digital Ionosonde: Design and Results, paper presented at 24th General Assembly of the International Union of Radio Science, Kyoto, Japan.

Makela, J. J., E. S. Miller, and E. R. Talaat (2010), Nighttime medium-scale traveling ionospheric disturbances at low geomagnetic latitudes, *Geophys*. *Res*. *Lett*., 37, L24104, doi:10.1029/2010GL045922.

Mannucci, A., B. Wilson, D. Yuan, C. Ho, U. Lindqwister, and T. Runge (1998), A global technique for GPS-derived ionospheric total electron content measurements, *Radio Sci*., 33, 565-582.

Maruyama, T., G. Ma, and M. Nakamura (2004), Signature of TEC storm on 6 November 2001 derived from dense GPS receiver network and ionosonde chain over Japan, *J. Geophys*. *Res*., 109, A10302, doi:10.1029/2004JA010451.

Mikhailov, A. V., A. K. Depueva, and T. Y. Leschinskaya (2004), Morphology of quiet time F2-layer disturbances: High to lower latitudes, *Int*. *J. Geomagn*. *Aeron*., 5, GI1006, doi:10.1029/2003GI000058.

Mikhailov, A. V., and M. Förster (1999), Some F2-layer effects during the 6-11 January CEDAR storm period as observed with the Millstone Hill Incoherent scatter facility, *J. Atmos*. *Terr*. *Phys*., 61, 249–261.

Mikhailov, A. V., M. Förster, and T. Y. Leschinskaya (2000a), On the mechanism of the post-midnight winter NmF2 enhancements: dependence on solar activity, *Ann*. *Geophys*., 18, 1422-1434.

Mikhailov, A. V., T. Yu. Leschinkaya, and M. Förster (2000b), Morphology of *Nm*F2 night-time increases in the Eurasian sector, *Ann*. *Geophys*., 18, 618–628.

Nicolls, M. J., M. C. Kelley, M. N. Vlasov, Y. Sahai, J. L. Chau, D. L. Hysell, P. R. Fagundes, F. Becker-Guedes, and W. L. C. Lima (2006), Observations and modeling of post-midnight uplifts near the magnetic equator, *Ann*. *Geophys*., 24, 1317-1331.

Oya, H., T. Takahashi, and S. Watanabe (1986), Observation of low latitude ionosphere by the impedance probe on board the Hinotori satellite, *J*. *Geomagn*. *Geoelectr*., 38, 111–123.

Pavlov, A. V., and N. M. Pavlova (2005), Mechanism of the post-midnight winter night-time enhancements in NmF2 over Millstone Hill during 14– 17 January 1986, *J*. *Atmos*. *Sol*. *Terr*. *Phys*., 67(4), 381 – 395, doi:10.1016/j.jastp.2004.11.004.

Pavlov, A. V., and N. M. Pavlova (2007), Anomalous nighttime peaks in diurnal variations of NmF2 close to the geomagnetic equator: A statistical study, *J*. *Atmos*. *Sol*. *Terr*. *Phys*., 69, 1871–1883, doi:10.1016/j.jastp.2007.07.003.

Pezzopane, M. (2004), Interpre: a Windows software for semiautomatic scaling of ionospheric parameters from ionograms, *Computers & Geosc*., 30, 125–130.

Pezzopane, M., and C. Scotto (2007), The automatic scaling of critical frequency foF2 and MUF(3000)F2: a comparison between Autoscala and ARTIST 4.5 on Rome data, *Radio Sci*. 42, RS4003. doi:10.1029/2006RS003581.

Pezzopane, M., E. Zuccheretti, C. Bianchi, C. Scotto, B. Zolesi, M. A. Cabrera, and R. G. Ezquer (2007), The new ionospheric station of Tucumán: first results, *Ann*. *Geophys*.-*Italy*, 50(3), 483-492.

Prölss, G. W. (1993), Common origin of positive ionospheric storms at middle latitudes and the geomagnetic activity effect at low latitudes, *J*. *Geophys*. *Res*., 98, 5981–5991.

Reinisch, B. W., I. A. Galkin, G. Khmyrov, A. Kozlov, and D. F. Kitrosser (2004), Automated collection and dissemination of ionospheric data from the digisonde network, *Adv. Radio Sci*., 2, 241-247.

Richards, P. G., M. Buonsanto, B. W. Reinisch, J. Holt, J. A. Fennely, J. A. Scali, R. H. Comfort, G. A. Germany, J. Spann, M. Brittnacher, and M. C. Fok (2000a), On the relative importance of convection and temperature to the behavior of the ionosphere in North America during January 6 – 12, 1997, *J*. *Geophys*. *Res*., 105, A6, doi:10.1029/1999JA000253.

Richards, P. G., T. Chang, and R. H. Comfort (2000b), On the causes of the annual variation in the plasmaspheric electron density, *J*. *Atmos*. *Sol*. *Terr*. *Phys*., 62, 935–946, doi:10.1016/S1364-6826(00)00039-0.

Rishbeth, H., and M. Mendillo (2001), Patterns of F2-layer variability, *J. Atmos. Terr. Phys.*, 63, 1661–1680, doi:10.1016/S1364-6826(01)00036-0.

Romano, V., S. Pau, M. Pezzopane, E. Zuccheretti, B. Zolesi, G. De Franceschi, and S. Locatelli (2008), The electronic Space Weather upper atmosphere (eSWua) project at INGV: advancements and state of the art, *Ann. Geophys.*, 26, 345-351.

Sastri, J. H. (1998), On the development of abnormally large postsunset upward drift of equatorial F region under quiet geomagnetic conditions, *J. Geophys. Res.*, 103, A3, doi:10.1029/97JA02649.

Scherliess, L., and B. G. Fejer (1997), Storm time dependence of equatorial dynamo zonal electric fields, *J. Geophys. Res.*, 102, A11, doi:10.1029/97JA02165.

Shiokawa, K., C. Ihara, Y. Otsuka, and T. Ogawa (2003), Statistical study of nighttime medium-scale traveling ionospheric disturbances using mid-latitude airglow images, *J. Geophys. Res.*, 108, 1052, doi:10.1029/2002JA009491.

Su, Y. Z., G. J. Bailey, and N. Balan (1994), Night-time enhancements in TEC at equatorial anomaly latitudes, *J. Atmos. Sol. Terr. Phys.*, 56, 1619–1628.

Titheridge, J. E. (1988), The real height analysis of ionograms: a generalized formulation, *Radio Sci.*, 5, 831–849.

Tsugawa, T., T. Otsuka, A. J. Coster, and A. Saito (2007), Medium-scale traveling ionospheric disturbances detected with dense and wide TEC maps over North America, *Geophys*. *Res*. *Lett*., 34, L22101, doi:10.129/2007GL031663.

Valladares, C. E., S. Basu, K. Groves, M. P. Hagan, D. Hysell, A. J. Mazzella Jr., and R. E. Sheehan (2001), Measurement of the latitudinal distributions of total electron content during equatorial spread F events, *J. Geophys*. *Res*., 106, A12, doi:10.1029/2000JA000426.

Valladares, C. E., J. Villalobos, R. Sheehan, and M. P. Hagan (2004), Latitudinal extension of low-altitude scintillations measured with a network of GPS receivers, *Ann*. *Geophys*., 22, 3155–3175.

Watanabe, S., and H. Oya (1986), Occurrence characteristics of low latitude ionospheric irregularities observed by impedance probe on board Hinotori satellite, *J. Geomagn*. *Geoelectr*., 38, 125–149.

Wakai, N., H. Ohyama, and T. Koizumi (1987), *Manual of Ionogram Scaling*, 3rd version, Radio Research Laboratory Ministry of Posts and Telecommunications, Japan.

Woodman, R. F. (1970), Vertical drift velocities and east-west electric fields at the magnetic equator, *J. Geophys*. *Res*., 75, 31, doi:10.1029/JA075i031p06249.

Zhao, B., W. Wan, L. Liu, K. Igarashi, M. Nakamura, L. J. Paxton, S. Y. Su, G. Li, and Z. Ren (2008), Anomalous enhancement of ionospheric electron content in the Asian-Australian region during a geomagnetically quiet day, *J. Geophys*. *Res*., 113, A11302, doi:10.1029/2007JA012987.

Figure 1. 3-hourly *Kp*, *Dst*, and *AE* indices from the 1st to the 8th of March 2010.

Figure 2. *fo*F2 measured values recorded at EACF mid-high latitude station on the 5th, 6th, and 7th of March 2010.

Figure 3. *fo*F2 plots obtained at (a) Jicamarca, (b) SL, (c) CP, (d) SJC, and (e) Tucumán on the 6th of March 2010. Lack of data at Jicamarca from 04:00 to 05:30 UT and at São José dos Campos from 02:00 to 05:30 UT is due to spread-F phenomena. Vertical grey lines at CP, SJC, and Tucumán highlight the occurrence time of the enhancement maximum.

Figure 4. *h*'F plots obtained at (a) Jicamarca, (b) SL, (c) CP, (d) SJC, and (e) Tucumán on the 6th of March 2010.

Figure 5. (a) Electron density variations for the real height range 170-300 km computed for the 6th of March 2010 from 00:00 to 10:00 UT, and (b) the corresponding enlargement from 05:00 to 09:00 UT. Oblique line highlights the downward phase shift typical of GW propagation.

Figure 6. Electron density profiles obtained at Tucumán on the 6th of March 2010 at 05:00, 06:30, 08:15, and 08:30 UT showing the compression and expansion phases of the F layer. At 06:30 UT the association between the *fo*F2 impulsive enhancement and the compression phase is clearly visible.

Figure 7. Virtual height variation for 2, 3, 4, 5, 6, and 7 MHz obtained at SJC on the 6th of March 2010 from 00:00 to 08:00 UT. Oblique line highlights the downward phase shift typical of GW propagation.

Figure 8. Two-dimensional maps of vTEC over an area extending in latitude from 0° S to 45° S and in longitude from 50° W to 80° W on the 6th of March 2010 from 04:30 to 07:00 UT with a 10 minute interval. Black solid circles in each plot represent the location of GPS receivers. Open circle represents the location of Tucumán. Colour scale is in TEC unit (10^{16} electrons/m^2). Coordinates are geographic.

Figure 9. Slab thickness calculated for Tucumán on the 6th of March 2010. Large compressions and expansions of the ionosphere are observed from 05:00 to 11:00 UT.

Figure 10. Zonal electric field (negative values indicate westward direction) recorded by the C/NOFS satellite on the 6th of March 2010, over an area extending from 12.3° N to 2.8° S in latitude and from 40° W to 90° W in longitude, in an altitude range from 530 to 818 km, from 00:00 to 05:00 LT averaging on ten-minute bins.

Figure 11. Wave front of a MSTID propagating northwest in the southern hemisphere at time t_1 and time $t_2 > t_1$.

Table 1. Coordinates of GPS receivers and ionosondes used in the study.

Location	Instrument	Geographical Coordinates	Magnetic Latitude	Local Time
Bogota, Colombia (BOGT)	GPS	4.6° N, 71.5° W	14.6° N	UT-5
Puerto Ayora, Ecuador (GLPS)	GPS	0.7° N, 90.3° W	10.2° N	UT-6
Portho Velho, Brazil (POVE)	GPS	8.7° S, 63.9° W	1.2° N	UT-4
Salvador, Brazil (SAVO)	GPS	12.9° S, 38.4° W	4.5° S	UT-3
Arequipa, Peru (AREQ)	GPS	16.5° S, 71.5° W	6.4° S	UT-5
Cachoeira Paulista, Brazil (CHPI)	GPS	22.7° S, 45.0° W	13.6° S	UT-3
Salta, Argentina (UNSA)	GPS	24.7° S, 65.4° W	14.6° S	UT-4
Curitiba, Brazil (UFPR)	GPS	25.4° S, 49.2° W	16.0° S	UT-3
Santiago, Chile (SANT)	GPS	33.2° S, 70.7° W	23.0° S	UT-5
San Martin, Argentina (BUE1)	GPS	34.6° S, 58.5° W	24.7° S	UT-4
La Plata, Argentina (LPGS)	GPS	34.9° S, 57.9° W	25.0° S	UT-4
Concepcion, Chile (CONZ)	GPS	36.8° S, 73.0° W	26.6° S	UT-5
Sao Luis, Brazil (SL)	DPS4	2.6° S, 44.2° W	6.2° N	UT-3
Jicamarca, Peru	DPS4	12.0° S, 76.8° W	2.0° S	UT-5
Cachoeira Paulista, Brazil (CP)	DPS4	22.4° S, 44.6° W	13.4° S	UT-3
São José dos Campos, Brazil (SJC)	CADI	23.2° S, 45.9° W	14.1° S	UT-3
Tucumán, Argentina	AIS-INGV	26.9° S, 65.4° W	16.8° S	UT-4

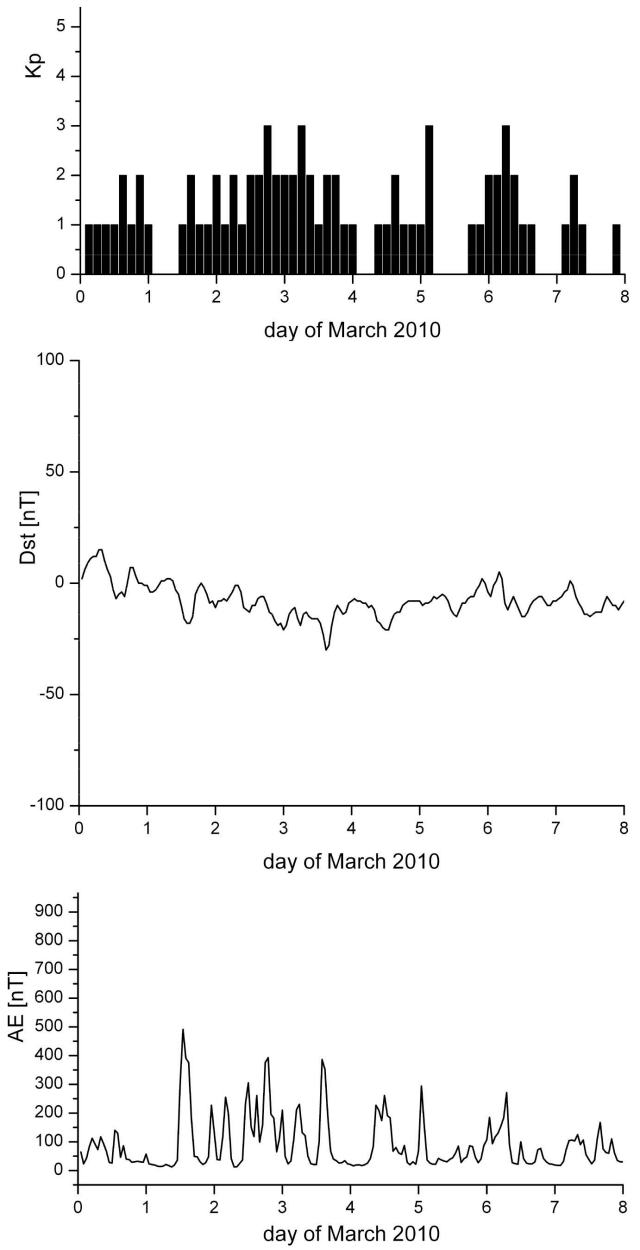
Kp
0
1
2
3
4
5
0
1
2
3
4
5
6
7
8
day of March 2010
Dst [nT]
100
50
0
-50
-100
0
1
2
3
4
5
6
7
8
day of March 2010
AE [nT]
0
100
200
300
400
500
600
700
800
900
0
1
2
3
4
5
6
7
8
day of March 2010

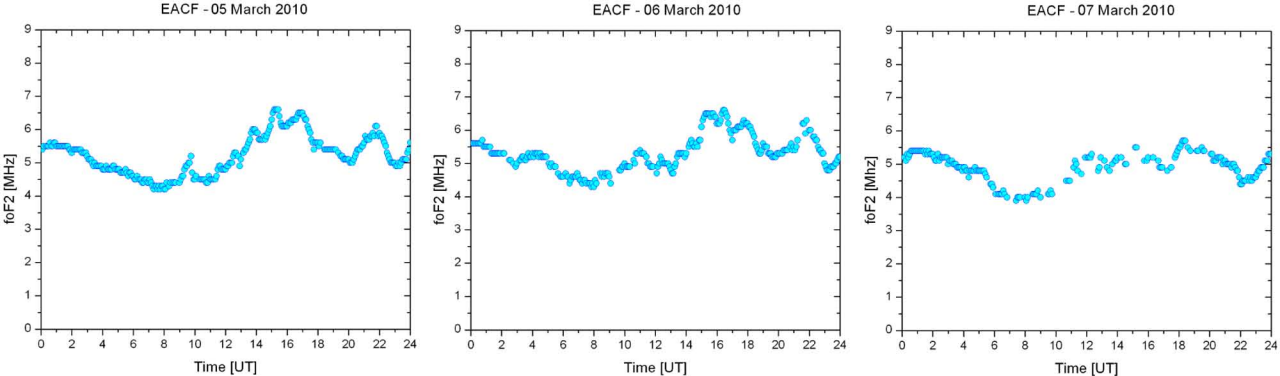
EACF - 05 March 2010
EACF - 06 March 2010
EACF - 07 March 2010
foF2 [MHz]
Time [UT]
0 1 2 3 4 5 6 7 8 9
0 2 4 6 8 10 12 14 16 18 20 22 24

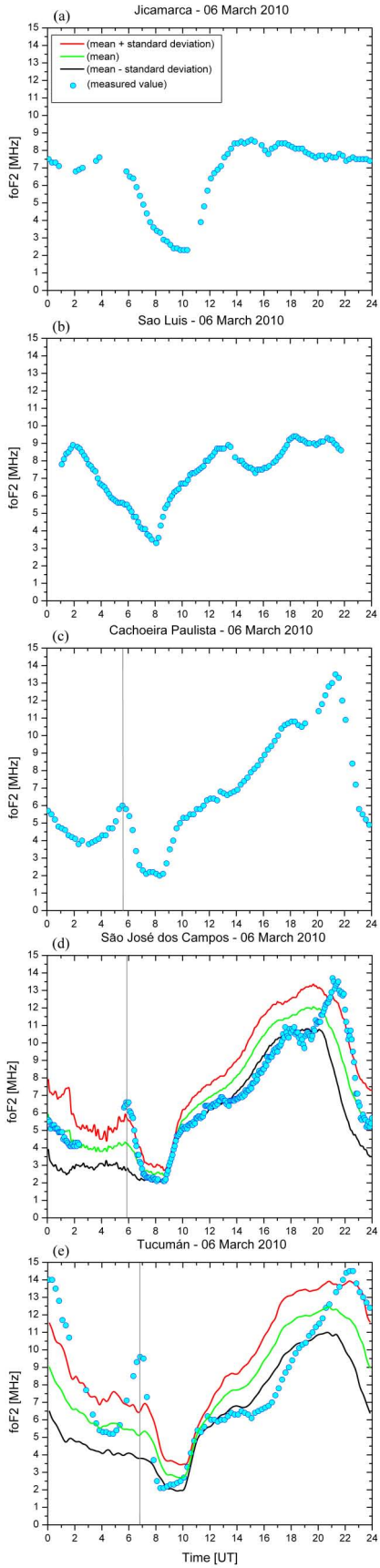
(a)
Jicamarca - 06 March 2010
(mean + standard deviation)
(mean)
(mean - standard deviation)
(measured value)
foF2 [MHz]
(b)
Sao Luis - 06 March 2010
foF2 [MHz]
(c)
Cachoeira Paulista - 06 March 2010
foF2 [MHz]
(d)
São José dos Campos - 06 March 2010
foF2 [MHz]
(e)
Tucumán - 06 March 2010
foF2 [MHz]
Time [UT]

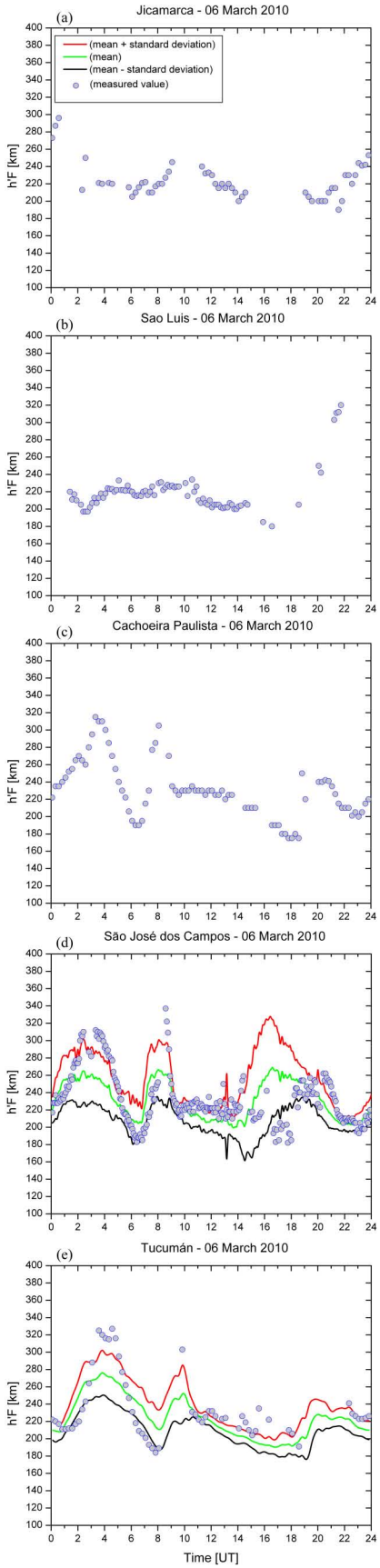
(a)
Jicamarca - 06 March 2010
(mean + standard deviation)
(mean)
(mean - standard deviation)
(measured value)
h'F [km]
(b)
Sao Luis - 06 March 2010
h'F [km]
(c)
Cachoeira Paulista - 06 March 2010
h'F [km]
(d)
São José dos Campos - 06 March 2010
h'F [km]
(e)
Tucumán - 06 March 2010
h'F [km]
Time [UT]

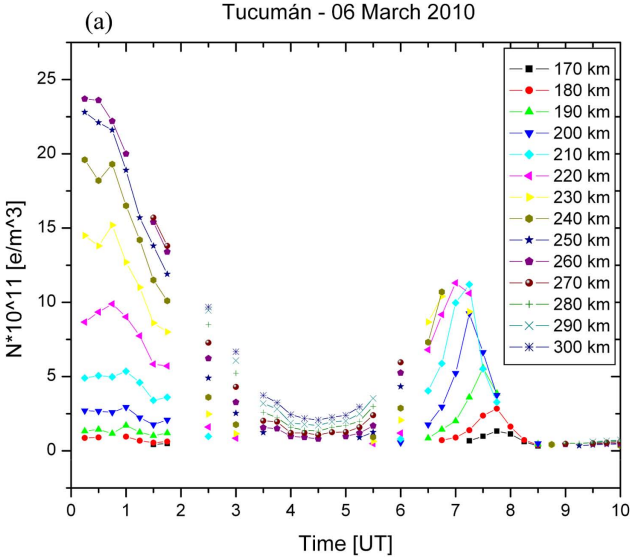
(a)
Tucumán - 06 March 2010
170 km
180 km
190 km
200 km
210 km
220 km
230 km
240 km
250 km
260 km
270 km
280 km
290 km
300 km
N*10^11 [e/m^3]
Time [UT]

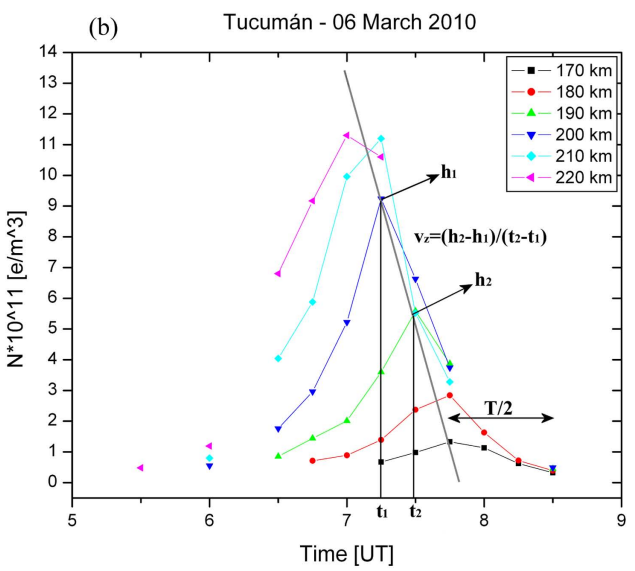
(b)
Tucumán - 06 March 2010
170 km
180 km
190 km
200 km
210 km
220 km
h1
vz=(h2-h1)/(t2-t1)
h2
T/2
t1
t2
N*10^11 [e/m^3]
Time [UT]

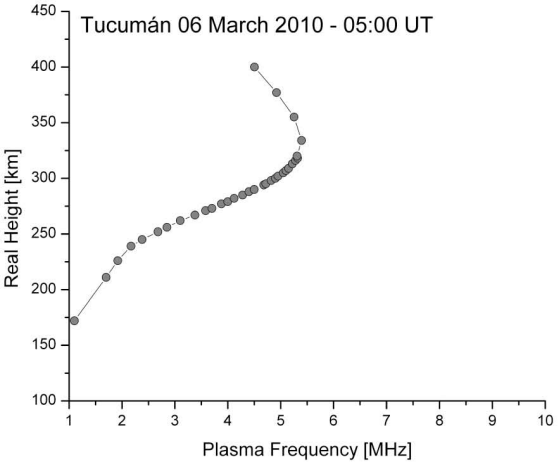
Tucumán 06 March 2010 - 05:00 UT
Real Height [km]
Plasma Frequency [MHz]

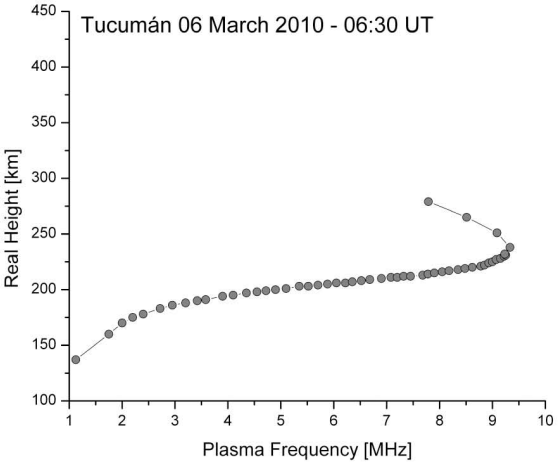
Tucumán 06 March 2010 - 06:30 UT
Real Height [km]
Plasma Frequency [MHz]

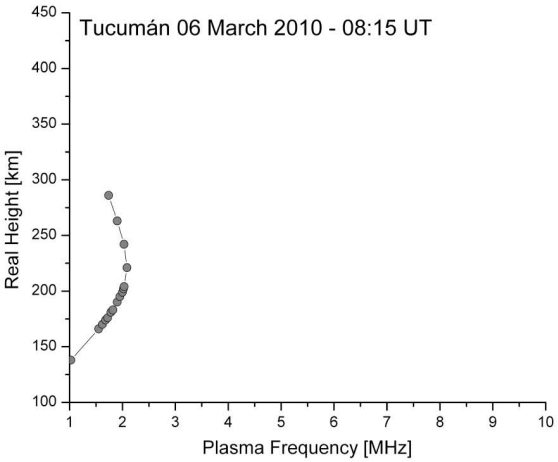
Tucumán 06 March 2010 - 08:15 UT
Real Height [km]
Plasma Frequency [MHz]

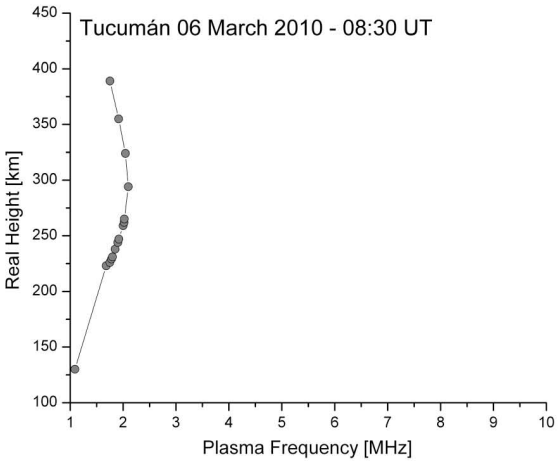
Tucumán 06 March 2010 - 08:30 UT
Real Height [km]
Plasma Frequency [MHz]

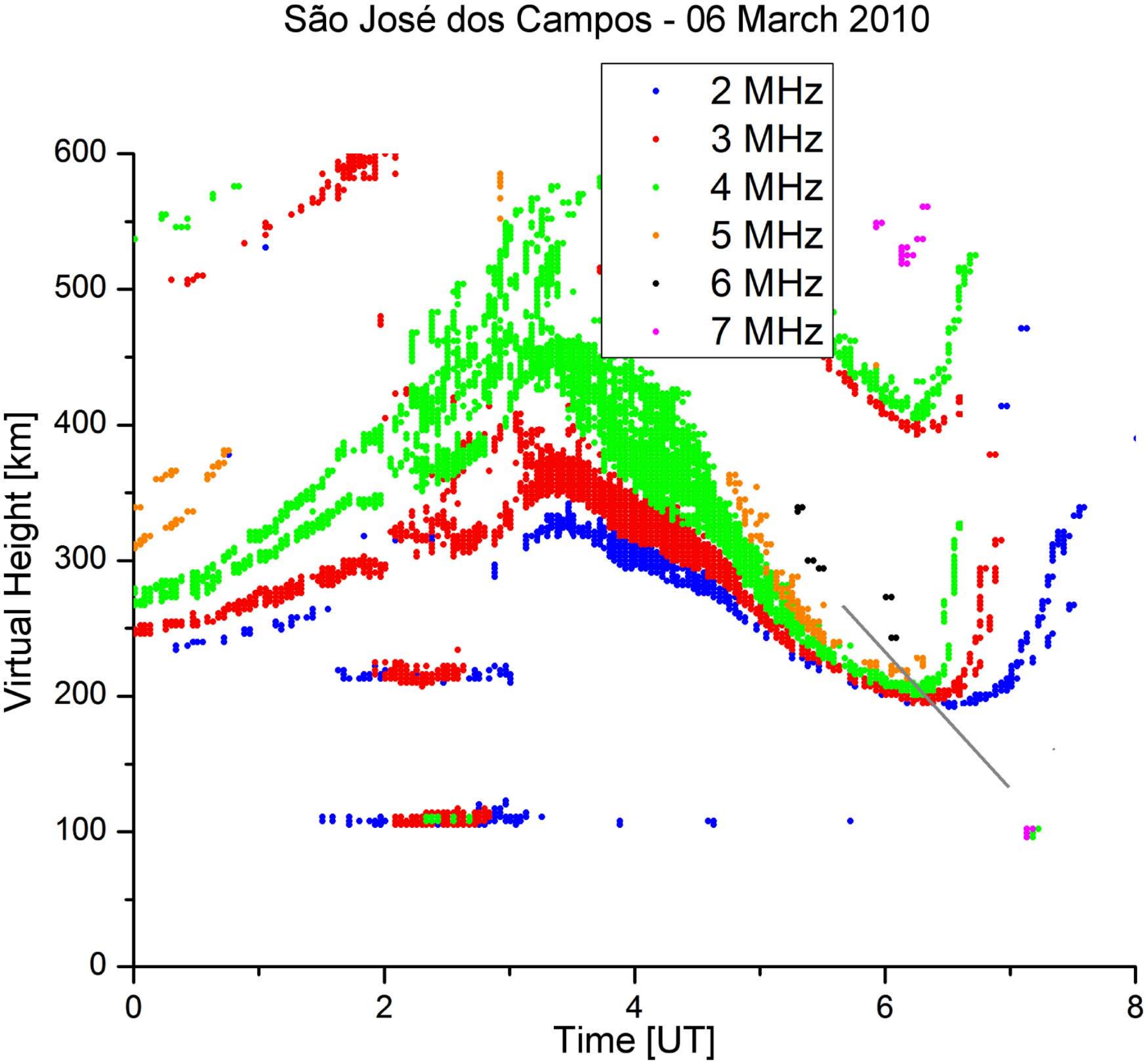
São José dos Campos - 06 March 2010
2 MHz
3 MHz
4 MHz
5 MHz
6 MHz
7 MHz
Virtual Height [km]
600
500
400
300
200
100
0
0
2
4
6
8
Time [UT]

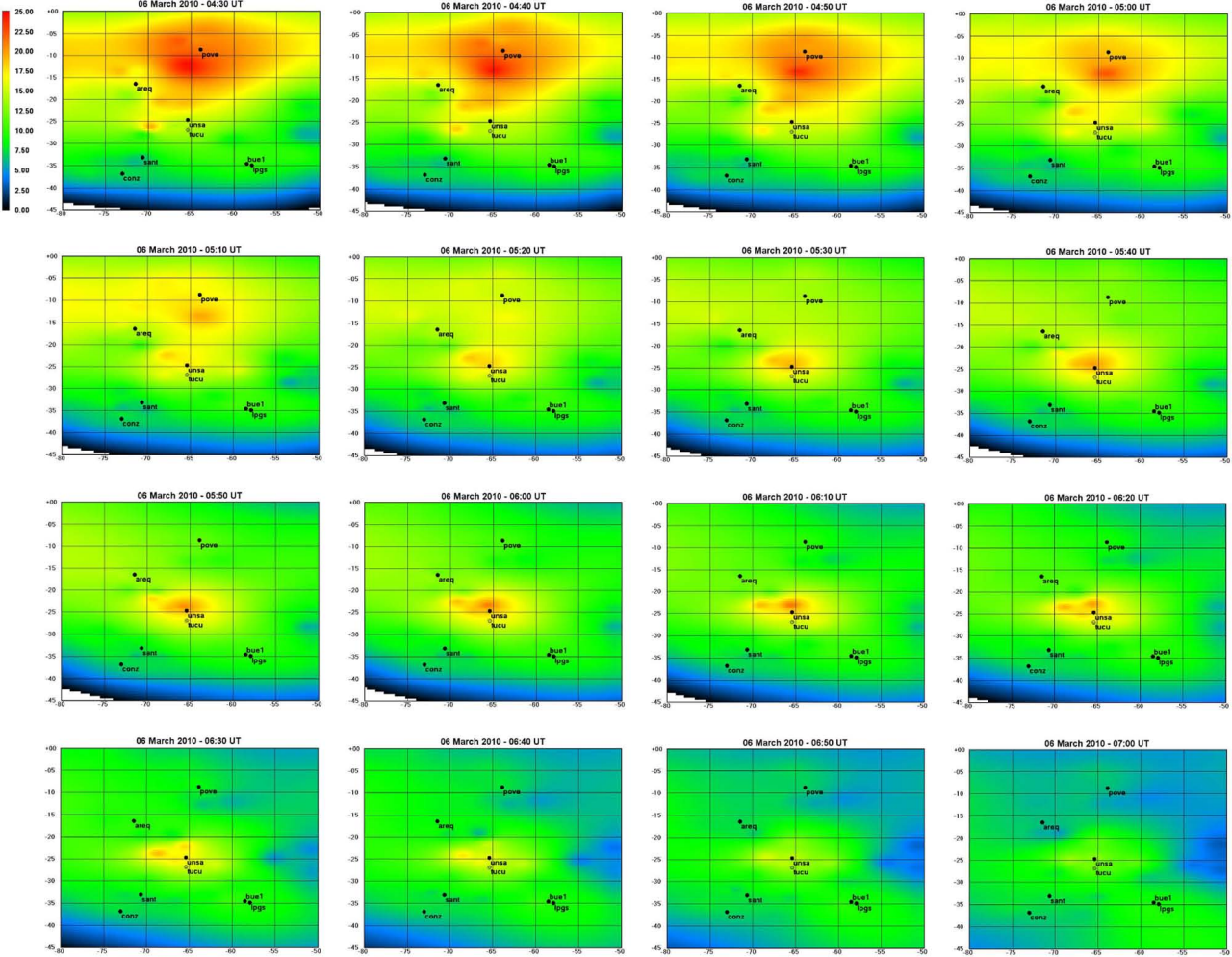
06 March 2010 - 04:30 UT
06 March 2010 - 04:40 UT
06 March 2010 - 04:50 UT
06 March 2010 - 05:00 UT
06 March 2010 - 05:10 UT
06 March 2010 - 05:20 UT
06 March 2010 - 05:30 UT
06 March 2010 - 05:40 UT
06 March 2010 - 05:50 UT
06 March 2010 - 06:00 UT
06 March 2010 - 06:10 UT
06 March 2010 - 06:20 UT
06 March 2010 - 06:30 UT
06 March 2010 - 06:40 UT
06 March 2010 - 06:50 UT
06 March 2010 - 07:00 UT
25.00
22.50
20.00
17.50
15.00
12.50
10.00
7.50
5.00
2.50
0.00
pove
areq
unsa
tucu
sant
conz
bue1
lpgs

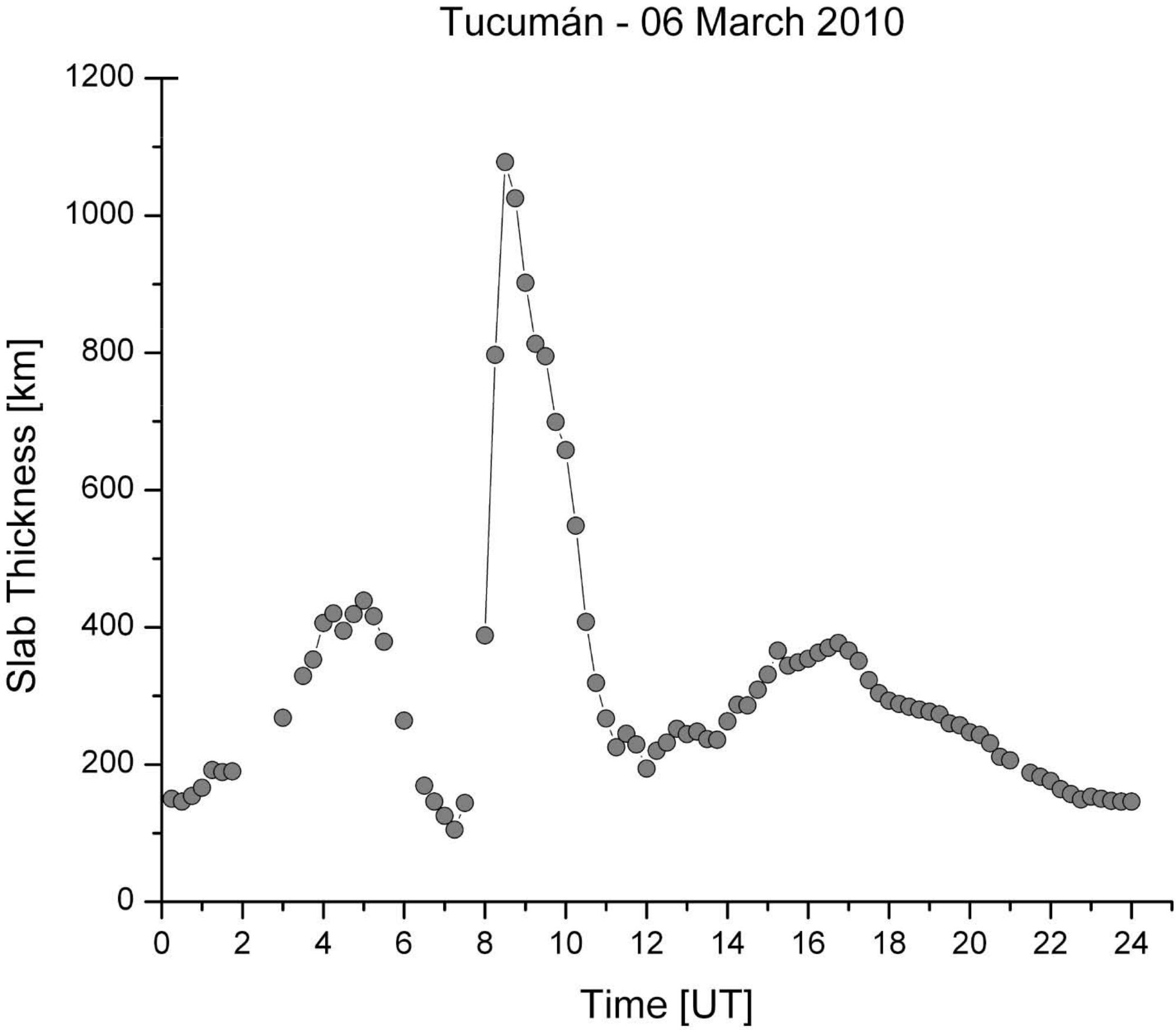
Tucumán - 06 March 2010
Slab Thickness [km]
Time [UT]
0
200
400
600
800
1000
1200
0
2
4
6
8
10
12
14
16
18
20
22
24

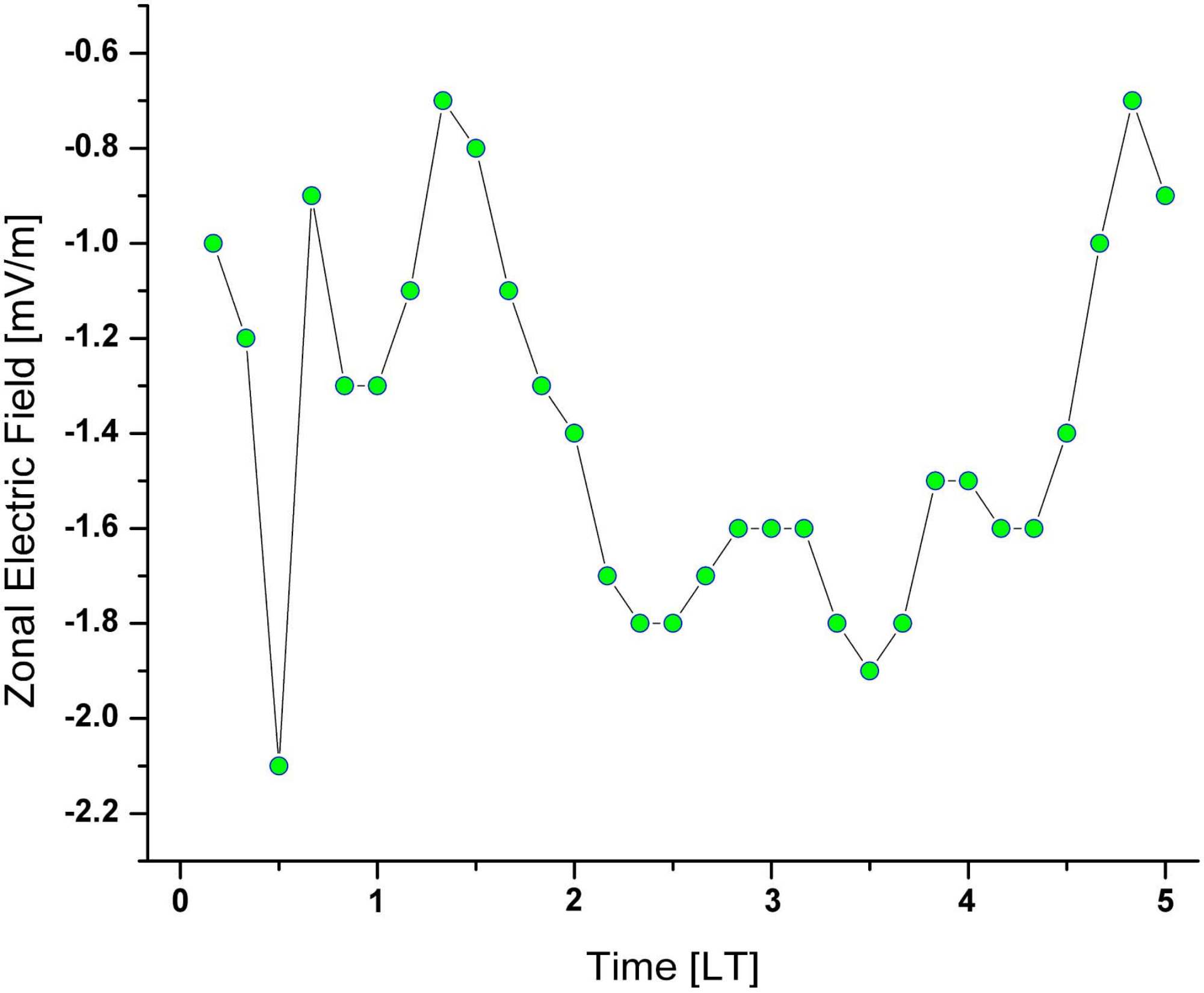
-0.6
-0.8
-1.0
-1.2
-1.4
-1.6
-1.8
-2.0
-2.2
Zonal Electric Field [mV/m]
0
1
2
3
4
5
Time [LT]


$t_2 > t_1$
t_1
Tucumán
~400 km
Cachoeira Paulista
São José dos Campos